The 2009 IEEE/RSJ International Conference on
Intelligent Robots and Systems
October 11-15, 2009 St. Louis, USA

An Experimental Study of Hierarchical Autopilot for Untrimmed Hingeless Helicopters

Tak-Kit Lau, Yun-hui Liu, *Fellow, IEEE* and Kai-wun Lin

Abstract— **Different from previous works that require prior trim conditions on the helicopter, this paper proposes a hierarchical PD controller that is robust in controlling untrimmed and therefore critically unstable helicopters. This controller can yield asymptotic stability of the helicopter in horizontal motion control, which can be proven by the linear stability analysis. And this controller can flawlessly engage with traditional dual loop autopilot by using auto-varying references in an inner stabilizing loop. Moreover, to facilitate the controller design, this paper derives the dynamics of hingeless helicopters with an emphasis on gyroscopic effect. Finally, the stability and superior performance of the proposed controller are empirically demonstrated on an instrumented JR Voyager GSR helicopter.**

I. INTRODUCTION

Unmanned aerial robots have been migrating from theoretical design to the practical use in recent decades [1]. The missions involving large-scale searching, tracking, rescuing in hostile environment require deploying dispensable yet promising aerial vehicles in an accurate and time-to-situation manner. Among other aerial robots, autonomous helicopters, especially the hobby-class ones, provide a better low-altitude maneuverability in terrain with obstacles, and safer recycle procedures upon mission, therefore they are especially more ideal for reconnaissance mission and narrow deployment environment. Yet, it also imposes challenge to the control of helicopters as the spatial buffer for correction of posture in flight are relatively limited in cases of sensor and mechanical failures, controller latency, and unmatched trimming values.

A. Prior Trimming

Normally helicopters and aircrafts are trimmed by experienced pilots before flight [2]. Some [3][4][5] attempted to control helicopters with a prior condition that the vehicle must be trimmed in advance. This equilibrium condition not only provides a configuration for nonlinear models to be linearized around certain values, it also leads to a convenient assumption that inner loop tracking references can be constant (Discussed in Section IV). However, due to the fact that the configuration changes from time to time on the vehicle (e.g. fuel consumption, wind gust, cargo deployment), the trim error will lead to significant stability issue and is often left to controllers to compensate [6]. Trimming and control is often studied separately, the obvious reason is that the aircraft can be trimmed by skilled pilots in advance, leading to a condition that gives a trimmed control input, the dynamics of the system converges to equilibrium. Other than manual trimming, some automatic trimming methods are proposed using interval analysis [7], ANN [8] and solving by closed-form equation [9]. Except being offline and therefore become inapplicable in certain circumstances, these methods, however, obtain accurate and unique trim values only if the system is thoroughly known. This paper proposes a method that is to auto-vary the tracking reference in the inner control loop, hence the helicopter can be controlled without a prior trimming condition, such that the helicopter does not require to be trimmed in advance for flight control.

This work was partially sponsored by the Hong Kong RGC under the grants 414406 and 414707. T.K. Lau, Y.H. Liu and K.W. Lin are with the Department of Mechanical and Automation Engineering, The Chinese University of Hong Kong, China. E-mail: {tklau,yhliu,kwlin}@mae.cuhk.edu.hk

Fig. 1. The instrumented JR Voyager GSR 260 under the governance of the proposed controller. The white bars below the landing gear were installed to avoid flapping during touch-down.

B. Hingeless Helicopter

For the type of helicopter, the model-sized hingeless helicopter has a rigid rotor system that provides feathering but no flapping [16], and hence it requires lesser components in the rotor design. Its high power-to-weight ratio and convenient availability enable this type of R/C helicopter to take up more loads and can be transformed to high performance and cost-efficient aerial robots. However, the simplicity of this kind of hingeless rotor design also leads to an unintuitive rotational dynamics through a series of servo motors and linkages for its actuation. This paper derives this actuation mechanism analytically to aid the controller design on this kind of helicopter.

II. INPUT-OUTPUT MECHANISM OF HINGELESS HELICOPTER

Hingeless helicopter is typically actuated through in total of five servomechanisms. Three for the swashplate, one for the engine's oil-air-mixture, and one for the tail pitch angle.

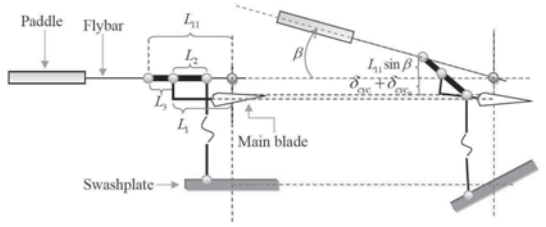

Fig. 2. The side-view of the rotor mechanism. The inputs from swashplate directly and indirectly influence the cyclic pitch angle via flybar and linkages. (Left) No inputs from swashplate; (Right) A flapping angle is generated by pulling the swashplate down.

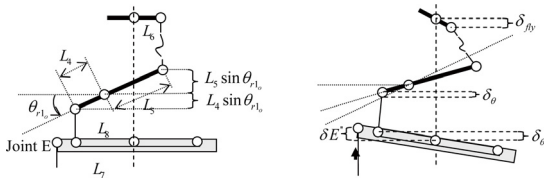

Fig. 3. The linkages from swashplate to paddle. (Left) The swashplate is horizontal and the resultant cyclic pitch angle is uniform in a revolution. (Right) Under the pitching backward command, the swashplate rotates and results in a non-zero flybar input (a.k.a. indirect input, δ_{fly}).

We derive and show the analytical form for the cyclic pitch angle, which is denoted as θ_{cyc}. It is heavily used in the next section.

A. Rotor Mechanism

The swashplate is a disc in the rotor that its outer ring links with three servomechanisms, namely elevator (front), aileron (port side) and pitch (starboard), and its inner circle on the upper side connects to a pair of four-bar-linkage mechanism. From the geometry shown in Fig. 2, we can readily obtain the cyclic pitch angle at an azimuth angle in a function of the direct input and flapping angle.

$$\theta_{cyc}(\psi_R) = \sin^{-1}\left[\left(\frac{L_2}{L_2+L_3}\right)\frac{(\delta_{cyc}+\delta_{cyc_o}+L_{11}S_\beta)}{L_1}\right] + \theta_{cyc_o} \quad (1)$$

Where $\theta_{cyc}(\phi_R)$ is the cyclic pitch angle at an azimuth angle ϕ_R, δ_{cyc} is the direct input, β is the paddle flapping angle. And δ_{cyc_0}, θ_{cyc_0} are the initial displacement and angle at which the throttle command is at initial zero, L_{11} is an auxiliary linkage length described in Fig. 2, and all other auxiliary linkage lengths to be mentioned are specified in figures without further inline descriptions. The influence of direct input can be written as,

$$\delta_{cyc}(\psi_R) = \delta_\phi \cos\psi_R + \delta_\theta \sin\psi_R + \delta_{cyc}^{thro} \quad (2)$$

Where δ_ϕ is the roll displacement input, δ_θ is the pitch displacement input, and is the displacement input due to throttle command. As mentioned, this displacement is equal to all three servomechanisms under the same throttle command. The flapping angle is characterized by the indirect input. Using geometry shown in Fig. 2,

$$\sin\beta = \delta_{fly}/L_6 \quad (3)$$

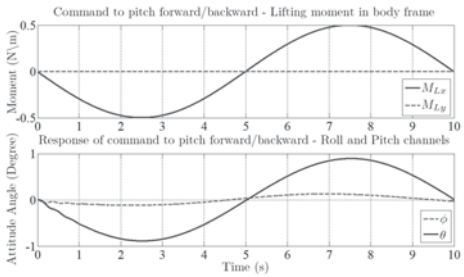

Fig. 4. The helicopter is commanded to pitch forward then backward. (Lower) The coupled dynamics is observed on the roll channel (dotted line).

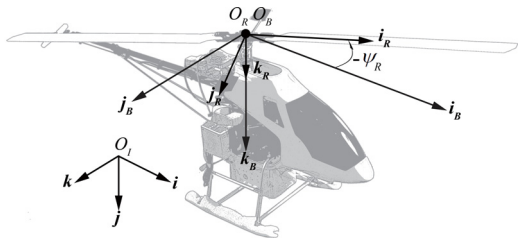

Fig. 5. The frame assignments on the helicopter. The body frame is attached on the fuselage, the rotor frame rotates with rotor and moves with body frame. The body x,y,z-axis are represented as directional unit vectors, namely i_B, j_B, k_B

Similarly, the indirect input can be found in this relation,

$$-(L_4\sin(-\theta_{r1}) - \delta_\theta)/L_4 = (L_5\sin\theta_{r1} - \delta_{fly})/L_5 \quad (4)$$

Such that,

$$\delta_{fly} = -L_5\delta_\theta/L_4 \quad (5)$$

In a revolution, we therefore obtain,

$$\delta_{fly}(\psi_R) = -L_5\left(\delta_\theta\sin\psi_R + \delta_\phi\cos\psi_R\right)/L_4 \quad (6)$$

B. Numerical analysis of cyclic pitch angle

Substituting (2) and (6) into (1), we can relate the roll and pitch inputs to the resultant cyclic pitch angle at an azimuth angle. From numerical results, we find it reasonable to approximate (1) by a Fourier series, such that,

$$\theta_{cyc}(\psi_R) \approx \delta_\phi a_{cyc}\cos\psi_R + \delta_\theta b_{cyc}\sin\psi_R + c_{cyc} \quad (7)$$

Where a, b, c_{cyc} are coefficients according to the instantaneous throttle command.

III. HELICOPTER DYNAMICS

The body frame of the helicopter is at the center of hub plane, namely hub point, and is shown in Fig. 5 along with other auxiliary frames.

$$\sum{}_I = \{i, j, k\} \quad (8)$$

$$\sum{}_B = \{i_B, j_B, k_B\} \quad (9)$$

$$\sum{}_R = \{i_R, j_R, k_R\} \quad (10)$$

In general, the helicopter dynamics can be expressed by,

$$\sum F = m\dot{v} + m\left(w \times v\right) \quad (11)$$

And by transport theorem [10],

$$\sum M = \dot{H} + w \times H \tag{12}$$

The term $\sum_F$ is the total external forces acting on the fuselage at hub point and is expressed in body frame; the velocity of the fuselage at hub point with respect to body frame is v, w is the angular velocity of fuselage at hub point with respect to inertial frame. For the rotational dynamics, H is the angular momentum of the fuselage, w is the angular velocity of the fuselage with respect to the inertial frame. The thrust generated by main blades can be written as,

$$T = -\left[\frac{n}{12\pi}\rho ca\Omega^2 (BR)^3 \int_0^{2\pi} \theta_{cyc} d\psi_R\right] k_B \tag{13}$$

Where n is the number of blades, ρ is the air density, c is the chord length, a is the lift curve slope, B is the tiploss factor [11], R is the length of a main blade and Ω is the spinning speed of main rotor, θ_{cyc} is the cyclic pitch angle, ϕ_R is the azimuth angle. The total external moments acting on the fuselage includes the moment due to the reaction of gyroscopic effect from the spinning rotor (M_G), uneven incremental lift along main blades (M_L), tail rotor thrust (M_t), deadweight (M_W), motor torque (M_M) and aerodynamic drag (M_D), such that,

$$\sum M = M_G + M_L + M_t + M_W + M_M + M_D \tag{14}$$

The aerodynamic moments can be derived readily from blade element theory in [12]. The aerodynamic drag,

$$M_D = \frac{n}{3}\rho ca\Omega^2 (BR)^3 k_B \tag{15}$$

The incremental lift along main blades,

$$M_L(\psi_R) = \frac{\rho ca\Omega^2 (BR)^4}{8\pi} \begin{pmatrix} -\int_0^{2\pi} \theta_{cyc}(\psi_R) S_{\psi_R} d\psi_B i_B \\ +\int_0^{2\pi} \theta_{cyc}(\psi_R) C_{\psi_R} d\psi_R j_B \end{pmatrix} \tag{16}$$

Where ϕ_R is the azimuth angle, its direction is shown in Fig. 5, and θ_{cyc} is the cyclic pitch angle of main blade. Similarly, the tail rotor thrust and its moment,

$$T_t = -\left(\frac{n_t}{6}\rho c_t a_t \Omega_t^2 \theta_{tail} (BR_t)^3\right) j_B \tag{17}$$

$$M_t = {}^B r_t \times T_t = \begin{bmatrix} \frac{r^B_{tz}}{6}\rho c_t a_t \Omega_t^2 \theta_{tail} (BR_t)^3 \\ 0 \\ -\frac{r^B_{tx}}{6}\rho c_t a_t \Omega_t^2 \theta_{tail} (BR_t)^3 \end{bmatrix} \tag{18}$$

Where ${}^B r_t$ is the position vector of the tail hub point with respect to body frame, θ_{tail} is the pitch angle of tail blade, R_t is the radius of tail blade, c_t is the chord length, a_t is the lift curve slope, and Ω_t is the spinning speed of the tail which can be obtained using gear ratio. The deadweight and the moment due to deadweight can be derived,

$${}^B W = mg\,[-\sin\theta \quad \sin\phi\cos\theta \quad \cos\phi\cos\theta\,] \tag{19}$$

$$M_w = {}^B r_{cg} \times {}^B W = \begin{bmatrix} mgC_\theta({}^B r^y_{cg} C_\phi - {}^B r^z_{cg} S_\phi) \\ mg(-{}^B r^z_{cg} S_\theta - {}^B r^x_{cg} C_\phi C_\theta) \\ mg({}^B r^x_{cg} S_\phi C_\theta + {}^B r^y_{cg} S_\theta) \end{bmatrix} \tag{20}$$

Where ${}^B W$ is the deadweight acting on the fuselage with respect to body frame, ${}^B r_{cg}$ is the position vector of the center of mass with respect to body frame, m is the mass of the helicopter, g is the gravity, $[\,\phi \quad \theta \quad \psi\,]^T$ are attitude angles, namely roll, pitch and yaw.

As the high-speed spinning rotor is the dominating factor over the rotational dynamics of helicopter, we can express the rotational dynamics of the rotor by transport theorem [10],

$${}^R M_G = \dot{H}_R + \omega_R \times H_R \tag{21}$$

Where ${}^R M_G$ is the moment acting on the rotor with respect to inertial frame and is expressed in the moving frame, $\sum_R$; H_R is the angular momentum of the rotor, w_R is the angular velocity of the rotor with respect to inertial frame. And using frame transformation, we have,

$$\begin{aligned} w_R &= \dot{\psi}_R k_R + \dot{\psi} k + \dot{\theta} j_1 + \dot{\phi} i_2 \\ &= \begin{bmatrix} \dot{\psi}\left(-C_{\psi_R} S_\theta + S_{\psi_R} S_\phi C_\theta\right) + \dot{\theta} S_{\psi_R} C_\phi + \dot{\phi} C_{\psi_R} \\ \dot{\psi}\left(S_{\psi_R} S_\theta + C_{\psi_R} S_\phi C_\theta\right) + \dot{\theta} C_{\psi_R} C_\phi - \dot{\phi} S_{\psi_R} \\ \dot{\psi}_R + \dot{\psi} C_\phi C_\theta - \dot{\theta} S_\phi \end{bmatrix} \end{aligned} \tag{22}$$

Where $\dot{\phi_R}$ is the rate of azimuth angle, $[\,\dot{\phi} \quad \dot{\theta} \quad \dot{\psi}\,]^T$ are rate of attitude angles, k_R is the z-axis of the frame $\sum_R$ attached on the spinning rotor; j_1 is the y-axis after rotation about z-axis of inertial frame by yaw, i_2 is the x-axis after rotation about y-axis of the first transition frame by pitch. Expanding (21) by substituting (22), we obtain the analytical form of the moment acting on the rotor. As the spinning rotor experiences a change of angular momentum due to the external moments such as lifting moment and moment of deadweight, by conservation of angular momentum [17], a moment is induced to counter-act this change. By a transformation using the azimuth angle, the induced moment acting on the fuselage can then be formed,

$$M_G = -\begin{bmatrix} C_{\psi_R} & S_{\psi_R} & 0 \\ -S_{\psi_R} & C_{\psi_R} & 0 \\ 0 & 0 & 1 \end{bmatrix} {}^R M_G \tag{23}$$

Where M_G is the gyroscopically induced moment acting on the fuselage by the rotor. Using MATLAB Simulink®, we model the system using (12), (16), (20) and (23), the response of the overall dynamics due to a lifting moment is obtained and shown in Fig. 4. It is therefore reasonable to simplify the induced moment by relating it to the lifting moment and form an approximated but more intuitive expression. Combing the roll and pitch inputs derived in (7), (23), and the numerical results obtained in Fig. 4, we re-write the sum of lifting moment and the gyroscopically induced moment as,

$$M_L + M_G = [\,K_{L1}\delta_\phi \quad K_{L2}\delta_\theta \quad 0\,]^T \tag{24}$$

Where $K_{L1,2}$ are coefficients that can be obtained in experiments.

IV. CONTROLLER DESIGN AND STABILITY ANALYSIS

Typical control of autonomous helicopter is to cascade the control into architecture with dual loop [1]. The inner loop stabilizes the attitude, the outer loop receives command for trajectory following. As a result, trim errors in the inner loop can lead to degraded performance of overall flight qualities. Many previous works [3][4][5] rely heavily on the prior trimming condition either by experienced pilots, or by prior trimming techniques [7][9]. Some treat the trim error

TABLE I

PARAMETERS FOR THE STABILITY ANALYSIS

Par.	Value	Unit	Par.	Value	Unit
m	11.2	kg	${}^{P}K_{vx,y}$	12.19,11.18	
I_{xx}	2.10	kgm^2	${}^{P}K_{\phi,\theta}$	48.37,51.80	
I_{xy}	0.96	kgm^2	${}^{D}K_{\phi,\theta}$	11.08,11.85	
I_{xz}	1.07	kgm^2	$K_{L1.2}$	1.14,1.98	
I_{yx}	0.96	kgm^2	$a_{vx,y}$	0.0057	
I_{yy}	3.68	kgm^2	${}^{B}r_{cg}$	[13 21 217.6]	mm
I_{yz}	2.83	kgm^2	$L_{1,2,3}$	31,17,16	mm
I_{zx}	1.07	kgm^2	$L_{4,5}$	13.68,22.8	mm
I_{zy}	2.83	kgm^2	$L_{4,7,8}$	19,38,19.4	mm
I_{zz}	4.02	kgm^2	$L_{9,11}$	34.6,50	mm

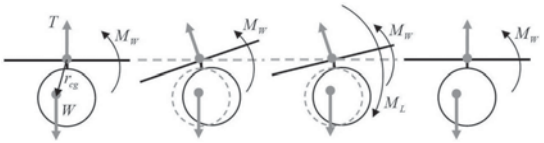

Fig. 6. (From left, 1) To consider the attitude along, the deadweight is not vertically under the hub point and it produces a moment with the position vector of center of gravity. (2) The moment due to deadweight rotates the vehicle and; (3) a feedback moment is generated as the state residual is not zero. As long as the gains of the control loop are large enough, the vehicle can be bought upright again such that the attitude is at desired state, [0 0]'. (4) However, as the residual is zero again, the net moment is unbalanced by the moment due to deadweight.

as uncertainty and control the helicopter by learning [13], adaptive control [6], and dynamic programming [14].

A. Design considerations

For hingeless helicopter, as shown in Section II, as long as the rotor is rigid, the direction of thrust is fixed and is always perpendicular to the hub plane, thus when the center of gravity of the vehicle is not directly below the spinning shaft, it leads to unstable performance and very often left to the outer loop to compensate (Fig. 6). A quick engineering fix is to carefully calibrate cargo and on-board equipment position in order to achieve a perfect configuration for the center of gravity, or to manually trim the vehicle before flight, or even avoid flights that need to change the loading during missions. In view of not limiting possible flight missions and lengthening pre-flight calibrations, and being able to flawlessly enhance the typical control scheme

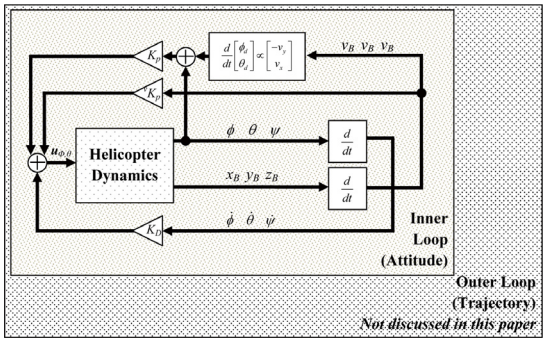

Fig. 7. The proposed controller.

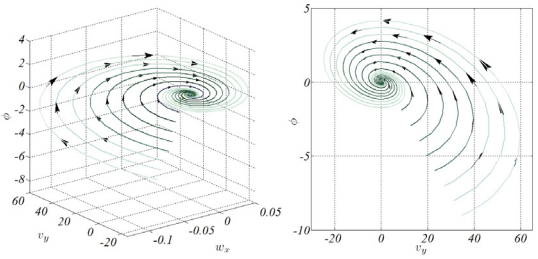

Fig. 8. (Left) The phase portrait on the roll channel of the vehicle under the governance of the proposed controller. (Right) From ϕ-v_y plane, it shows more clearly that the spiral node converges even at a largely biased initial attitude (up to about 10^o), such that the proposed controller can still stabilize the attitude and hence the horizontal motion by using inner loop alone.

on helicopter, the proposed controller hierarchically varies the tracking reference in typical inner attitude control loop in order to stabilize the dynamics.

B. Controller design

The complete model is described by,

$$f(x, u, \Theta) = \dot{x} \tag{25}$$

Where x is the state, u is the control input, and Θ is the trim condition. Using state-space representation,

$$\dot{x} = Ax + Bu \tag{26}$$

$$y = Cx$$

Where A, B, C are typical state matrixes. Solving the trim condition is equivalent to solving the nonlinear equation in (25). Our consideration in this control problem is that the helicopter is not trimmed in advance. Therefore we write,

$$f(x_e, u_e, 0) \neq 0 \tag{27}$$

Where u_e is the control input with prior trim conditions. Our objective is to design a controller for hingeless helicopter and achieve an asymptotically stability without trimming the helicopter,

$$\forall \delta > 0, \lim_{t \to 0} x(t) = 0 \text{ with } \|x(t_0)\| < \delta x \in^n \tag{28}$$

Where δ is the perturbation. The feedback is written as the conventional negative state feedback,

$$u = -Kx \tag{29}$$

C. Hierarchy of the varying tracking reference

We propose a controller that varies the tracking reference in order to stabilize the attitude of the hingeless helicopter. This proposed controller focuses on enhancing the stability of the inner loop of typical dual loop autopilot, therefore we use a PI controller to stabilize the yaw channel, and only the throttle is manually controlled. For the feedback gain matrix in (29),

$$K = \begin{bmatrix} 0 & {}^{P}K_{v_y} & {}^{D}K_{\phi} & 0 & {}^{P}K_{\phi} & 0 & -{}^{P}K_{\phi} & 0 \\ -{}^{P}K_{v_x} & 0 & 0 & {}^{D}K_{\theta} & 0 & {}^{P}K_{\theta} & 0 & -{}^{P}K_{\theta} \end{bmatrix} \tag{30}$$

The state vector is now written as $[\, v_x \quad v_y \quad w_x \quad w_y \quad \phi \quad \theta \quad \phi_d \quad \theta_d \,]^T$.

The proportional (P) control inside the inner loop and the tuning of its tracking reference forms a hierarchy that the controller can adapt to the state variations due to the untrimmed conditions. In general, the vehicle drifts to the direction in which the tracking reference is not biased to. Therefore, the rate of change of the tracking reference is negatively proportional to the tendency of motion of the vehicle, that is equivalent to its geometrical velocity in the body frame,

$$\frac{d}{dt}\begin{bmatrix}\phi_d\\ \theta_d\end{bmatrix} \propto \begin{bmatrix}-v_y\\ v_x\end{bmatrix} \tag{31}$$

Substituting (29) into (26), the stability can be analyzed by solving this differential equation,

$$\dot{x} = (A - BK)\,x \tag{32}$$

Substituting (15), (18), (20), (24) into (14) from the previous sections, we have the rotational dynamic model of the hingeless helicopter,

$$M_G + M_L + M_t + M_W + M_M + M_D = \dot{H} + w \times H \tag{33}$$

As mentioned, the rotational dynamics is controlled by a PI controller, therefore, we can explicitly set the sum of tail, motor and drag moments to zero. Using first order Taylor expansion, we can linearize the model at certain operating state x_o,

$$\begin{bmatrix}\delta\dot{x}_1\\ \vdots\\ \delta\dot{x}_n\end{bmatrix} = \begin{bmatrix}\frac{\partial f_1(x_o,u_o)}{\partial x_1} & \cdots & \frac{\partial f_1(x_o,u_o)}{\partial x_n}\\ \vdots & \ddots & \vdots\\ \frac{\partial f_n(x_o,u_o)}{\partial x_1} & \cdots & \frac{\partial f_n(x_o,u_o)}{\partial x_n}\end{bmatrix}\begin{bmatrix}\delta x_1\\ \vdots\\ \delta x_n\end{bmatrix} \tag{34}$$

Where u_o is the control input without trim condition. The solution to the differential equation in (32) can then be written in this form,

$$\delta x_i = c_1^i V_1^i e^{\lambda_1^i t} + c_2^i V_2^i e^{\lambda_1^i t} + \cdots + c_n^i V_n^i e^{\lambda_1^i t}, i \in [1, n] \tag{35}$$

Where c, V, λ are constants, eigenvectors and eigenvalues of solutions to the differential equation in (25), and n is the number of states. As mentioned, the interest at the moment is to control horizontal motion by considering rotational dynamics, and the yaw channel is well-controlled by a PI controller, we can let alone the yaw channel, and diminish the states into $[\,u \quad v \quad p \quad q \quad \phi \quad \theta \quad \phi_d \quad \theta_d\,]^T$ only. This state representation includes the trim states in (31). We can perform partial derivative on (11), (26), (33) in (34) with respect to each state, and obtain the model in state-space representation,

$$\begin{bmatrix}\dot{u}\\ \dot{v}\\ \dot{p}\\ \dot{q}\\ \dot{\phi}\\ \dot{\theta}\\ \dot{\phi}_d\\ \dot{\theta}_d\end{bmatrix} = \begin{bmatrix}0 & r_0 & 0 & -w_0 & 0\\ -r_0 & 0 & w_0 & 0 & g\cos\phi_0\cos\theta_0\\ 0 & 0 & B_1 & B_3 & B_5\\ 0 & 0 & B_2 & B_4 & B_6\\ 0 & 0 & 1 & \frac{\sin\theta_0\sin\phi_0}{\cos\theta_0} & B_7\\ 0 & 0 & 0 & \cos\phi_0 & -q_0(\sin\phi_0)\\ a_{vy} & 0 & 0 & 0 & 0\\ 0 & a_{vx} & 0 & 0 & 0\end{bmatrix}$$
$$\begin{bmatrix}-g\cos\theta_0 & 0 & 0\\ -g\sin\phi_0\sin\theta_0 & 0 & 0\\ B_8 & 0 & 0\\ B_9 & 0 & 0\\ B_{10} & 0 & 0\\ 0 & 0 & 0\\ 0 & 0 & 0\\ 0 & 0 & 0\end{bmatrix}\begin{bmatrix}u\\ v\\ p\\ q\\ \phi\\ \theta\\ \phi_d\\ \theta_d\end{bmatrix} + \begin{bmatrix}0 & 0\\ 0 & 0\\ \frac{K_{L1}}{I_x} & 0\\ 0 & \frac{K_{L2}}{I_y}\\ 0 & 0\\ 0 & 0\\ 0 & 0\\ 0 & 0\end{bmatrix}\begin{bmatrix}\delta_\phi\\ \delta_\theta\end{bmatrix} \tag{36}$$

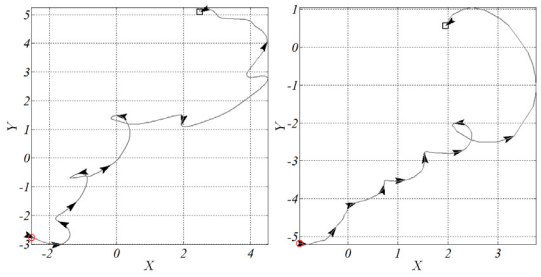

Fig. 9. Experimental results of a typical inner loop PID controller which failed even after several trials of tuning. The units in each axis are meters. Duration: (Left) 19.2s, (Right) 22.6s. This controller activated at the circled point. It first stopped the vehicle from moving but it drifted over time. It failed to stabilize the vehicle. (Refer to the enclosed video clip, part 1)

$$\begin{aligned}
B_1 &= \frac{-I_{zx}q_0 + I_{yx}r_0}{I_x}\\
B_2 &= \frac{I_{zy}q_0 - (I_x - I_z)r_0 + 2I_{zx}p_0}{I_y}\\
B_3 &= \frac{-I_{zx}p_0 - (I_z - I_y)r_0 - 2I_{zy}q_0}{I_x}\\
B_4 &= \frac{-I_{xy}r_0 + I_{zy}p_0}{I_y}\\
B_5 &= \frac{mg\cos\theta_0(-r_y\sin\phi_0 - r_z\cos\phi_0)}{I_x}\\
B_6 &= \frac{mg(r_x\sin\phi_0\cos\theta_0)}{I_y}\\
B_7 &= (\sin\theta_0\cos\phi_0/\cos\theta_0)\,q_0\\
B_8 &= \frac{-mg\sin\theta_0(r_y\cos\phi_0 - r_z\sin\phi_0)}{I_x}\\
B_9 &= \frac{mg(-r_z\cos\theta_0 + r_x\cos\phi_0\sin\theta_0)}{I_y}\\
B_{10} &= q_0\left(\sin\phi_0\sec^2\theta_0\right)
\end{aligned}$$

D. Asymptotical stability and robustness

From (35) and (36), we can evaluate the stability by examining whether all its real parts are negative. Using the model parameters in Table I, we can readily find that all the eigenvalues have negative real parts.

$$\begin{aligned}
\lambda_\phi &= -1.9996 \pm 5.0531i,\ -1.9802,\ -0.0250\\
\lambda_\theta &= -1.8799 \pm 4.5688i,\ -2.5695,\ -0.0461
\end{aligned} \tag{37}$$

The phase portrait in Fig. 8 shows how this controller can guarantee a stable spiral node for a small perturbation away from equilibrium, such that the states converge. Using linear stability analysis, as all eigenvalues have negative real parts, the solutions to the differential equation in (35) converge, and hence an asymptotical stability is proved [15]. The robustness of the proposed controller is evaluated in terms of phase margin. It is the difference between -180^o and the phase at the frequency in which the magnitude of the transfer function of the system crosses 0dB. The guaranteed bound of phase margin is obtained by method of balancing the sensitivity function of the transfer matrix (Implemented as a function embedded in MATLAB Robust Control Toolbox™). This controller exhibits a remarkable phase margin of $\pm 82^o$.

V. EXPERIMENTS

The controller is extensively tested on the JR Voyager GSR260 hobby-class helicopter which is of hingeless type.

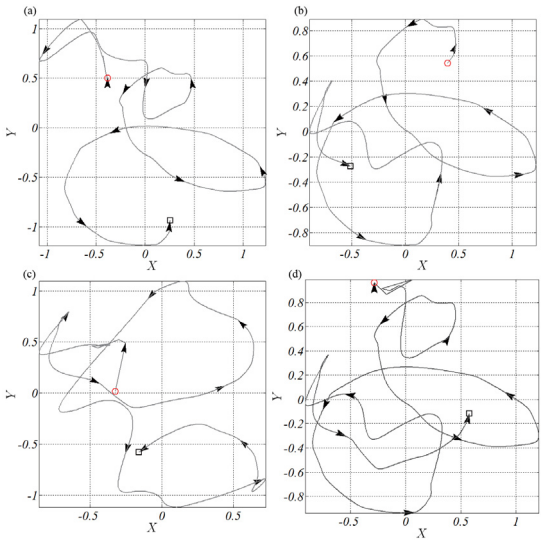

Fig. 10. Experimental results of the proposed controller. The units on each axis are meters. The durations: (a) 19.71s (b) 16.40s (c) 13.91s, and (d) 25.01s. The mean absolute displacements (in meters): [0.41 0.51], [0.52 0.43], [0.68 0.88], and [0.43 0.45]. The proposed controller constrains the movement within a bounded area of about $1m^2$ (Refer to the enclosed video clip, part 2)

Its weight is 11.2kg, length 1.48m and height 0.67m. We use XSens IMU to measure the angular velocity and attitude. The geometric data are collected from NovAtel RT2 GPS card, the accuracy is up to $\pm$2cm at 20Hz sampling rate as long as the satellite coverage is sufficient. The vehicle carries a mini-pc during the flight, and the processor is of Intel Atom™1.6GHz. All processing are completed on-board. No data fusion algorithm such as Kalman filter is implemented in order to maintain a low-computational cost for future migration to low-performance processing units. First, a typical inner loop PID attitude controller was tested on the platform. After several trials on different gains, it still could not stabilize the dynamics; it acted virtually as a PD controller such that the severe horizontal drifting demonstrates that this controller cannot stabilize the helicopter of hingeless type in which the thrust is always perpendicular to the hub plane. The untrimmed conditions (for example, due to biased center of gravity, $\left\| r_{cg} \times [0 \quad 0 \quad mg]^T \right\| > 0$) leads to unstable hovering of the vehicle. In principle PID controller can stabilize the vehicle, but in practice we found that it is more difficult to have it properly tuned than our proposed controller. The proposed controller was then tested on the same platform. The results shown in Fig. 10 are coherent with the expectation, and it successfully constrains the horizontal movement of the untrimmed vehicle within a bounded area of about $1m^2$.

VI. CONCLUSION

The purpose of this study is to show that it is possible to utilize a simple hierarchical PD controller on a hingeless helicopter for the horizontal movement control. We prove the asymptotical stability of this control scheme using linear stability analysis, and validate in field using an instrumented JR Voyager GSR helicopter. The advantage of this simple controller is that this control scheme is remarkably robust in terms of phase margin, and can be more easily tuned compared with typical PID controller for untrimmed helicopters. More, it requires neither optimal state estimation filters, nor prior trimming conditions of the helicopter. The experiments further demonstrate that the proposed controller can constrain the horizontal movement of an untrimmed helicopter in a bounded area of about a meter square under a windy condition.

VII. ACKNOWLEDGMENT

The first author would like to thank Mr. SONG Baoquan for the design and development of the first generation flight system for experiments, and to Mr. MOK Allan Wai-kit for the technical support.

REFERENCES

[1] K.P. Valavanis, *Advances in Unmanned Aerial Vehicles*. Netherlands: Springer, 2007, pp. 3-5.
[2] M. V. Cook, *Flight Dynamics Principles: A Linear Systems Approach to Aircraft Stability and Control.*, Burlington: Elsevier, 2007, pp. 32-39.
[3] A.C.B. Dimanlig, E.T. Meadowcroft, R. Strawn, M. Potsdam, "Computational Modeling of the CH-47 Helicopter in Hover," *in Proc. DoD High Performance Computing Modernization Program Users Group Conf.*, Washington, 2007, pp. 98-103.
[4] A. Yue, "Design of robust multivariable helicopter control laws for handling qualities enhancement," *in Proc. International Conf. on Control*, Oxford, 1988, pp. 689-694.
[5] M. Trentini, J.K. Pieper, "Model-Following Control of a Helicopter in Hover," *in Proc. IEEE International Conf. on Control Applications*, Dearborn, 1996, pp. 7-12.
[6] A.S. Krupadanam, A.M. Annaswamy, and R.S. Mangoubi, "A Multivariable Adaptive Controller for Autonomous Helicopters," *in Proc. of the American Control Conf.*, 2052-2057, 2002.
[7] E. van Kampen, Q.P. Chu and J.A. Mulder, "Nonlinear Aircraft Trim using Interval Analysis," *presented at AIAA GN&C Conf. and Ex.*, Hilton Head, South Carolina, Aug. 20-23, 2007, AIAA-2007-6766
[8] R. Enns, J. Si, "Helicopter Trimming and Tracking Control Using Direct Neural Dynamic Programming," *in Proc. of International Joint Conf. on Neural Networks*, vol.2, 1019-1024, 2001.
[9] M. R. Elgersma, B. G. Morton, "Nonlinear Six-Degree-of-Freedom Aircraft Trim," *AIAA J. of GC&D*, vol.23 no.2 pp. 305-311, 2000.
[10] F.P. Beer, E.R. Johnston, W.E. Clausen, G.H. Staab, *Vector Mechanics for Engineers: Dynamics.* McGraw-Hill Professional, 2003, pp.942-944, 1146-1150.
[11] W. Johnson, *Helicopter Theory.* Princeton U. Press, 1980, pp. 133.
[12] J.G. Leishman, *Principles of Helicopter Aerodynamics.* Cambridge U. Press, 2000, pp. 117-119.
[13] C.L. Bottasso, L. Riviello, "Trim of rotorcraft multibody models using a neural-augmented model-predictive auto-pilot," *J. of Multibody System Dynamics*, vol. 18, no. 3, pp. 299-321, 2007.
[14] R. Enns, J. Si, "Helicopter Trimming and Tracking Control Using Direct Neural Dynamic Programming," *in Proc. of International Joint Conf. on Neural Networks*, vol. 2, pp.1019-1024, 2001.
[15] M. Tabor, *Chaos and integrability in nonlinear dynamics.* New York: Wiley, 1988, pp. 20-25.
[16] Federal Aviation Administration, *Rotorcraft Flying Handbook*. New York: Skyhorse Publishing, 2007, pp. 13
[17] B.Siciliano, O.Khatib, *Springer Handbook of Robotics*. Springer, 2008, pp.480